Published OnlineFirst April 27, 2010; DOI: 10.1158/1535-7163.MCT-09-1061

Research Article

Molecular Cancer Therapeutics

Inhibition of Fatty Acid Synthase Suppresses c-Met Receptor Kinase and Induces Apoptosis in Diffuse Large B-Cell Lymphoma

Shahab Uddin[1], Azhar R. Hussain[1], Maqbool Ahmed[1], Rong Bu[1], Saeeda O. Ahmed[1], Dahish Ajarim[2], Fouad Al-Dayel[3], Prashant Bavi[1], and Khawla S. Al-Kuraya[1]

Abstract

Fatty acid synthase (FASN), the enzyme responsible for *de novo* synthesis of fatty acids, has emerged as a potential therapeutic target for several cancers; however, its role in diffuse large B-cell lymphoma (DLBCL) has not been fully elucidated. In this study, we investigated the role of FASN in a large series of DLBCL tissues in a tissue microarray (TMA) format followed by *in vitro* studies using DLBCL cell lines. FASN was found to be expressed in 62.6% DLBCL samples and was seen in highly proliferative tumors, manifested by high Ki67 ($P < 0.0001$). Significant association was found between tumors expressing high FASN and c-Met tyrosine kinase ($P < 0.0002$), as well as p-AKT ($P = 0.0309$). *In vitro*, pharmacological FASN inhibition and small interference RNA (siRNA) targeted against FASN triggered caspase-dependent apoptosis and suppressed expression of c-Met kinase in DLBCL cell lines, which further highlighted the molecular link between FASN and c-Met kinase. Finally, simultaneous targeting of FASN and c-Met with specific chemical inhibitors induced a synergistically stimulated apoptotic response in DLBCL cell lines. These findings provide evidence that FASN, via c-Met tyrosine kinase, plays a critical role in the carcinogenesis of DLBCL and strongly suggest that targeting FASN may have therapeutic value in treatment of DLBCL. *Mol Cancer Ther; 9(5); 1244–55. ©2010 AACR.*

Introduction

Diffuse large B-cell lymphoma (DLBCL) is a common and heterogeneous lymphoid malignancy (1). Although subsets of patients with DLBCL are cured with combination chemotherapy, significant proportions of DLBCL patients are refractory to chemotherapy and eventually die of the disease. Therefore, a better understanding of the molecular and cellular heterogeneity of DLBCL will lead to the discovery of potential therapeutic targets.

Fatty acid synthase (FASN) is a multifunctional enzyme that catalyzes the terminal steps in the synthesis of the 16-carbon fatty acid palmitate in cells (2, 3). In normal cells, FASN expression levels are relatively low, because fatty acid is generally supplied by dietary fatty acid. In contrast, FASN is expressed at significantly higher levels in a variety of human epithelial cancers including breast, thyroid, colon, ovary, lung, and prostate (4–11). Overexpression of FASN has also been reported in hematological malignancies including leukemia and multiple myeloma (11–13). Moreover, several reports have shown that FASN expression levels correlate with tumor progression, aggressiveness, and metastasis (6, 7). For example, FASN expression levels are predictive of poor prognosis in breast and prostate cancer (7). As FASN has been strongly linked to tumor cell proliferation (6), and is preferentially expressed in cancer cells, it represents an attractive target for novel anticancer therapy (7, 11).

Recent studies have suggested that there is a functional interaction between FASN enzymatic activity and different receptor tyrosine kinases (RTK) such as HER2 and c-Met (14, 15). RTKs and their specific ligands are essential components of intracellular signaling pathways used for the control of growth, differentiation, and survival. One of the RTKs that has been implicated in playing a major role in tumorigenesis is c-Met and its ligand hepatocyte growth factor (HGF). Uncontrolled activation of the HGF/c-Met kinase signaling pathway has been implicated in tumor growth, invasion, and metastasis (16). Several studies suggested a strong pathogenic role for c-Met via the PI3-kinase/AKT signaling pathway in a variety of tumors including DLBCL (17, 18).

Authors' Affiliations: [1]Human Cancer Genomic Research, King Fahad National Center for Children's Cancer and Research, Research Center, [2]King Faisal Cancer Centre, [3]Department of Pathology, King Faisal Specialist Hospital and Research Center, Riyadh, Saudi Arabia

Note: Supplementary material for this article is available at Molecular Cancer Therapeutics Online (http://mct.aacrjournals.org/).

S. Uddin and A.R. Hussain are joint first authors.

Corresponding Author: Khawla S. Al-Kuraya, Department of Human Cancer Genomic Research, King Fahad National Center for Children's Cancer & Research, King Faisal Specialist Hospital and Research Cancer, MBC#98-16, P.O. Box 3354, Riyadh 11211, Saudi Arabia. Phone: 966-1-205-5167; Fax: 966-1-205-5170. E-mail: kkuraya@kfshrc.edu.sa

doi: 10.1158/1535-7163.MCT-09-1061

Published OnlineFirst April 27, 2010; DOI: 10.1158/1535-7163.MCT-09-1061

Because FASN has been shown to have a critical role in carcinogenesis and progression of several human cancers, exploration of its role in DLBCL can lead to new therapeutic targets to improve survival. Therefore, in this study we sought to test the hypothesis that increased FASN activity plays an active role in DLBCL tumorigenesis. Our study shows that in clinical samples, FASN is linked with c-Met expression, suggesting a possible role in DLBCL tumorigenesis. We show that FASN-dependent signaling regulates the expression of c-Met RTK in DLBCL. We further show that pharmacological and small interference RNA (siRNA)-mediated inhibition of FASN negatively regulates the expression of c-Met. Altogether, our data show that downregulation of c-Met expression, because of FASN inhibition, shows a novel link between FASN activity and c-Met expression in DLBCL. Finally, these data suggest a possible potential role of FASN as a novel therapeutic target for the treatment of DLBCL.

Materials and Methods

Construction of tissue microarray. Tissue microarrays (TMA) were constructed as described previously (19). Briefly, three tissue cylinders with a diameter of 0.6 mm were punched from 301 DLBCL patients' archival paraffin blocks and transferred into a recipient paraffin block using a semi-automatic precision instrument (Beecher Instruments).

Patient samples. Three hundred and one cases of *de novo* DLBCL diagnosed between 1987 and 2006, and reclassified according to the World Health Organization criteria (20), were collected from the Department of Pathology at the King Faisal Specialist Hospital and Research Centre. Archival paraffin blocks and clinical data were obtained by reviewing the charts, according to the regulations of the hospital institutional review board. Patients were staged by means of computerized imaging and bone marrow biopsy. Of the 301 cases, 171 were nodal lymphomas and 130 were extranodal lymphomas. The institutional review board of King Faisal Specialist Hospital & Research Center approved the study.

Immunohistochemistry. TMA slides were processed and stained manually. The immunohistochemistry (IHC) protocol was followed as mentioned earlier (21). The streptavidin-biotin peroxidase technique with diaminobenzidine as chromogen was applied. The primary antibodies were diluted in a 1% solution of bovine serum albumin in PBS and incubated overnight at room temperature. Primary antibodies used, their dilutions, and cutoff levels for evaluation are listed in Supplementary Table S1. For antigen retrieval, Dako Target Retrieval solution pH 9.0 (catalog number S2368) was used, and the slides were microwaved at 750 W for 5 minutes and then at 250 W for 20 minutes. The Dako Envision Plus System kit was used as the secondary detection system with DAB as chromogen. All slides were counterstained with hematoxylin, dehydrated, cleared, and mounted. Negative controls included replacement of the primary antibody with no reacting antibodies of the same species. Only fresh cut slides were stained simultaneously to minimize the influence of slide ageing and maximize reproducibility of the experiment.

Immunohistochemistry assessment. FASN expression was categorized by doing an H score (5, 22). Each TMA spot was assigned an intensity score from 0 to 3 (I0, I1-I3), and proportion of the tumor staining for that intensity was recorded in 5% increments from a range of 0 to 100 (P0, P1-P3). A final H score (range 0-260) was obtained by adding the sum of scores obtained for each intensity and proportion of area stained (H score = I1×P1 + I2×P2 + I3×P3). X-tile plots were constructed for the assessment of biomarker and optimization of cutoff points on the basis of outcome as has been described earlier. X-tile plots are created by dividing marker data into three populations: low, middle, and high (i.e., two divisions). We used X-tile version 3.6.1 to define the optimal cutoff point for the negative and positive scores for FASN. On a training set of patients (n = 129) generated by the program, the greatest difference in linear survival trends was achieved comparing scores 0 to 10 versus 20 to 260 (χ^2 = 0.2767, P = 0.5839). This X-tile–determined cutoff was confirmed on the validation set (n = 130; χ^2 = 0.8328, P = 0.3711). This algorithm uses a training validation approach to define optimal prognostic cutoffs from continuous or ordinal tumor biomarker scoring data. Using this approach, scores of 0 to 10 were defined as FASN low and 20 to 260 as FASN high. Similarly, X-tile was used to define a cutoff point for c-Met overexpresssion.

p-AKT scoring was done as described earlier (23, 24). Briefly, *p*-AKT was scored as levels on an intensity scale ranging from 0 to 3. Scoring was done as follows: 0, no appreciable staining in tumor cells; 1, barely detectable staining in tumor cells; 2, appreciable staining of moderate intensity, distinctly marking tumor cells; and 3, readily appreciable staining of strong intensity. For purposes of statistical analysis, all cases staining at level 0 or 1 were grouped as *p*-AKT negative and all cases staining at level 2 and level 3 were grouped as *p*-AKT positive. The expression of CD10, BCL6, and MUM1, was considered to classify tumors as germinal center B-cell (GC) like DLBCL and activated B-cell (ABC), applying the decision tree described earlier (25–27). For each case, the core with the highest percentage of tumor cells stained was used for analysis.

Statistical analysis. The software used for statistical analysis was Statview 7.0 (SAS Institute Inc.). χ^2 tests were used to examine relationship between nominal variables. The limit of significance for all analyses was defined as a P-value of 0.05; two-sided tests were used in all calculations.

Cell culture. The human DLBCL cell lines SUDHL4, SUDHL5, and SUDHL10 were obtained from Deutsche Sammlung von Mikroorganismen und Zellkulturen (DSMZ), Braunschweig, Germany. The cell lines were cultured in RPMI 1640 medium supplemented with 20% (v/v) fetal bovine serum, 100 U/mL penicillin,

Published OnlineFirst April 27, 2010; DOI: 10.1158/1535-7163.MCT-09-1061

100 U/mL streptomycin at 370°C in an humidified atmosphere containing 5% CO2. All the experiments were done in RPMI-1640 containing 5% serum.

Reagents and antibodies. MTT and Bax (6A7) antibody were purchased from Sigma. C-75 and LY294002 were purchased from Calbiochem. c-Met inhibitor PHA665752 was purchased from Tocris Bioscience. Antibodies against *p*-AKT, caspase-9, *p*-Bad, *p*-FOXO-1, *p*-GSK3, FOXO-1, GSK-3, AKT, cleaved caspase-3, and Bid antibodies were purchased from Cell Signaling Technologies. c-Met and *p*-Met antibodies were purchased from Biosource. FASN, cytochrome c, beta-actin, caspase-3, and poly(ADP-ribose) polymerase (PARP) antibodies were purchased from Santa Cruz Biotechnology, Inc. XIAP, cIAP-1, survivin, and caspase-8 antibodies were purchased from R&D. Annexin V was purchased from Molecular Probes. Apoptotic DNA-ladder kit was obtained from Roche.

Cell cycle analysis, annexin V staining, and DNA laddering. DLBCL cell lines were treated with different concentrations of C-75 as described in the legends. For cell cycle analysis, cells were washed once with PBS and resuspended in 500 μL hypotonic staining buffer and analyzed by flow cytometry as described previously (28–30). For detection of apoptosis, cells were harvested and percentage apoptosis was measured by flow cytometry after staining with flourescein-conjugated annexin V and propidium iodide (Molecular Probes) and DNA laddering using a 1.5% agarose gel as described previously (31).

Cell lysis and immunoblotting. Cells were treated with C-75 as described in the legends and lysed as previously described (32). Briefly, following treatment, cell pellets were resuspended in phosphorylation lysis buffer on ice for 1 hour, spun at 14,000 RPM for 15 minutes, and supernatant was collected. Protein concentrations were assessed by Bradford assay before loading the samples. A total of 15 to 20 μg of proteins were separated by SDS-PAGE and transferred to polyvinylidene difluoride membrane (PVDF; Immobilon, Millipore). Proteins were immunoblotted with different antibodies and visualized by the enhanced chemiluminescence (Amersham) method.

Preparation of cytoplasmic and nuclear extracts. Nuclear extracts were prepared according to an earlier study (31). Briefly, 2 × 106 cells were washed with cold PBS and suspended in 0.4 ml hypotonic lysis buffer containing protease inhibitors for 30 minutes. The cells were then lysed with 10% NP-40. The homogenate was centrifuged, and supernatant containing the cytoplasmic extracts was stored frozen at −800°C. The nuclear pellet was resuspended in 25 μL ice-cold nuclear extraction buffer. After 30 minutes of intermittent mixing, the extract was centrifuged, and supernatants containing nuclear extracts were secured. The protein content was measured by the Bradford method. If the nuclear extracts were not used immediately, they were stored at −800°C.

Measurement of mitochondrial potential and cytochrome C release. After treatment of DLBCL cell lines with C-75 for 24 hours, mitochondrial membrane potential was measured using JC1 dye and release of cytochrome c was analyzed using immunoblotting of mitochondrial and cytosolic protein fractions as described previously (33).

Detection of Bax conformational changes. Cells were treated with indicated doses of C-75 and lysed with Chaps lysis buffer [10 mM HEPES (pH 7.4), 150 mM NaCl, 1% Chaps] and immunoprecipitated with anti-Bax 6A7 monoclonal antibody and Bax conformation was detected as described earlier (29).

Gene silencing using siRNA. FASN siRNA, (catalog number SI00059752 and SI00059759) and scrambled control siRNA were purchased from Qiagen (Valencia). Cells were transfected using lipofectamine 2000 (Invitrogen) for 6 hours following which the lipid and siRNA complex was removed and fresh growth medium was added. Cells were lysed 48 hours after transfection, and specific protein levels were determined by Western blot analysis with specific antibodies.

Results

FASN expression and its correlation with p-AKT and other clinicopathological parameters. High levels of FASN expression were seen in 62.6% (162 of 259) of the DLBCL patient samples (Fig. 1). The incidence of expression for other IHC markers is presented in Supplementary Table S1. As shown in Table 1, FASN overexpression was significantly associated with overexpression of *p*-AKT ($P = 0.0309$), c-Met ($P = 0.0002$), and Ki-67 ($P < 0.0001$). Interestingly, FASN overexpression was significantly more common in the GC subtype of DLBCL as compared with ABC subtype ($P = 0.0122$), and was also more common in females ($P = 0.0026$). However, FASN overexpression was not associated with age, stage, lactate dehydrogenase (LDH) level, International Prognostic Index (IPI), and overall survival ($P = 0.2888$). High levels of c-Met expression was seen in 73.2% (186/254) of the DLBCL samples and was associated with overexpression of FASN ($P = 0.0002$), *p*-AKT ($P = 0.0274$), and Ki-67 ($P = 0.0012$). DLBCL patients with overexpression of c-Met had a better overall survival of 76.2% at 5 years as compared with 57.5% ($P = 0.0028$) with low c-Met expression. In the multivariate analysis using Cox proportional hazard model for both factors, IPI, and c-Met, the relative risk was 2.33 for low c-Met expression [95% confidence interval (CI) 1.12-4.70; $P = 0.0241$] and 4.30 for high risk IPI group (95% CI 2.11-9.14; $P \leq 0.0001$). Thus c-Met overexpression was an independent prognostic marker for better survival in multivariate analysis (Supplementary Table S2).

FASN inhibition causes a dose-dependent inhibition of proliferation and apoptosis in DLBCL cell lines. We initially sought to determine whether treatment with a FASN-specific inhibitor, C-75, leads to inhibition of cell proliferation in DLBCL cells. DLBCL cell lines SUDHL4, SUDHL5, and SUDHL10 were cultured in the presence

Published OnlineFirst April 27, 2010; DOI: 10.1158/1535-7163.MCT-09-1061

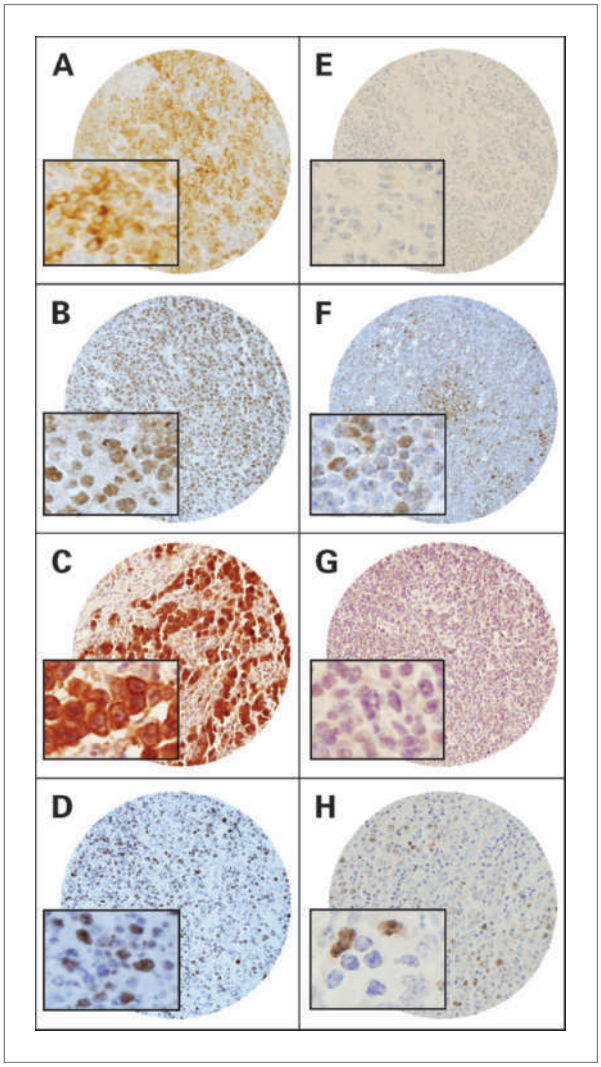

Figure 1. TMA-based IHC analysis of FASN and *p*-AKT in DLBCL patients. A DLBCL array spot showing: A, overexpression of FASN; B, c-Met; C, *p*-AKT; and D, Ki-67. In contrast, another DLBCL tissue array spot showing: E, low expression of FASN; F, c-Met; G, *p*-AKT; and H, Ki-67. The 20 × 0.70 objective on an Olympus BX 51 microscope (Olympus America Inc) with the inset showing a 40 × 0.85-aperture magnified view of the same.

of 10, 25, 50, and 100 μM C-75 for 24 hours, and cell proliferation was assayed using MTT assays. Figure 2A shows that as the dose of C-75 increased from 10 to 100 μM, cell growth inhibition increased in a dose-dependent manner in all the DLBCL cell lines. The growth inhibition induced by C-75 treatment was found to be statistically significant ($P < 0.01$; Student's *t*-test) at most of the doses tested in all cell lines.

In subsequent experiments, we determined whether the observed suppressive effects of C-75 in MTT assays are due to induction of cell cycle arrest or apoptosis. DLBCL cell lines were treated with C-75 for 24 hours and cell cycle fractions were determined. As shown in Fig. 2B, after 24 hours treatment, there was a substantial increase in the G2/M population in all cell lines at 25 μM of C-75. G2/M population increased from 15.11% in an untreated sample to 23.11% at 25 μM treatment in the SUDHL4 cell line, from 09.14 to 33.68% in the SUDHL5 cell line, and from 9.88 to 30.60% in the SUDHL10 cell line. Interestingly, at 50 μM C-75, the sub-G1 population of cells increased from 0.61 to 57.84% in SUDHL4, from 1.07 to 45.02% in SUDHL5, and from 1.38 to 38.53% in SUDHL10 cell lines, respectively (Fig. 2B). This increase in the sub-G1 population was accompanied by loss in G0/G1, S, and G2/M phases in treated cells, suggesting that cells are dying due to apoptosis. We also used annexin V/PI dual staining and DNA laddering for confirmation of C-75–induced apoptosis in DLBCL cells. Cells were treated with 25 and 50 μM C-75 for 24 hours, and apoptosis was measured by annexin V/PI dual staining. As shown in Fig. 2C, treatment of DLBCL cells with 25 and 50 μM C-75 induced 68% and 80% apoptosis in the SUDHL4, 63% and 75% in the SUDHL5, and 52% and 64% in the SUDHL10 cell lines, respectively. We analyzed DNA fragmentation, which is another hallmark of apoptosis. As shown in Fig. 2D, C-75 caused a dose-dependent DNA fragmentation in DLBCL cell lines. To confirm these results, we also treated SUDHL4 and SUDHL5 cell lines with 5 and 10 μg cerulenin, a naturally occurring inhibitor of FASN, and as shown in Supplementary Fig. S1A and B, cerulenin treatment caused an increase in the sub-G1 population of cells as detected by cell cycle analysis and induced apoptosis at both concentrations. These data suggest that FASN inhibition by C-75 and cerulenin induces apoptosis in DLBCL cell lines.

Constitutive expression of FASN associated with c-Met signaling pathways in DLBCL cell lines. High levels of FASN expression have been reported in a variety of solid tumors as well as in hematological malignancies (4–13). FASN has also been shown to regulate the activation of c-Met and AKT in other cancers (15). However, the relationship between FASN expression and activation of c-Met and AKT has not been fully elucidated in DLBCL. Using the DLBCL cell lines, we sought to determine the expression of FASN, *p*-Met, c-Met, and *p*-AKT, and their response to C-75 treatment. As shown in Fig. 3A, all DLBCL cell lines expressed constitutive FASN, *p*-Met and *p*-AKT (untreated cells), and treatment of DLBCL cells with C-75 suppressed FASN expression and dephosphorylated constitutively active *p*-Met and AKT. The level of c-Met protein was also suppressed following treatment with 25 and 50 μM C-75. In addition, treatment of DLBCL cell lines with C-75 also inhibited constitutively phosphorylated FOXO1 and GSK3; the downstream targets of AKT pathway (Supplementary Fig. S2). These data suggest that FASN-mediated growth and proliferation involves c-Met and AKT-mediated signaling in DLBCL cells.

We did transfection studies with siRNA specifically targeted against FASN to determine the status of these proteins in DLBCL cell lines. SUDHL4 and SUDHL5 cells were transfected with FASN-specific siRNA (catalog

Published OnlineFirst April 27, 2010; DOI: 10.1158/1535-7163.MCT-09-1061

Table 1. Correlation between FASN expression and clinicopathological features in DLBCL patients

Patient characteristics	Total		Overexpression		Reduced and/or absent		*P*
	No.	%	No.	%	No.	%	
No. of Patients	259		162	62.6	97	37.4	
Age (y)							
≤60	168	64.9	105	62.5	63	37.5	0.9826
>60	91	35.1	57	62.6	34	37.4	
Sex							
Female	108	41.7	79	73.1	29	26.9	0.0026
Male	151	58.3	83	55.0	68	45.0	
Performance Status*							
0-2	101	59.1	68	67.3	33	32.7	0.5461
3-4	70	40.9	44	62.9	26	37.1	
Stage*							
I-II	89	52.0	62	69.7	27	30.3	0.2325
III-IV	82	48.0	50	61.0	32	39.0	
Extranodal*							
One site	95	55.6	58	61.0	37	39.0	0.1700
More than one site	76	44.4	54	71.0	22	29.0	
LDH (IPI)*,†							
Normal (<480)	83	48.5	52	62.6	31	37.4	0.4470
High (>480)	88	51.5	60	68.2	28	31.8	
IPI Group*							
Low to low intermediate	114	66.7	75	65.8	39	34.2	0.9095
High intermediate to high	57	33.3	37	64.9	20	35.1	
GC versus ABC							
ABC	205	80.4	122	59.5	83	40.5	0.0122
GC	50	19.6	39	78.0	11	22.0	
p-AKT‡							
High (2, 3)	109	42.8	77	70.6	32	29.4	0.0309
Low (0-1)	146	57.2	84	57.5	62	42.5	
Ki-67‡							
>0	162	62.8	117	72.2	45	27.8	<0.0001
≤50	96	37.2	45	46.9	51	53.1	
c-Met‡							
Any one high	182	74.0	128	70.3	54	29.7	0.0002
Both low	64	26.0	28	43.8	36	56.2	
5-y overall survival				75.2		67.3	0.2888

NOTE: *p*-AKT, Ki-67, and cMET data were not available in all 259 cases with FASN information. Analysis failure of some markers for these IHC markers was attributed to missing or nonrepresentative spots.

*IPI information was only available in 171 patients.

†LDH categorization is based on the range of normal values in the clinical laboratory at our institution.

‡Although incidence of c-Met was 70.3%, 246 DLBCL spots were informative for both FASN and cMET expression. There were 4 DLBCL spots with cMET scores but noninformative for FASN.

number SI00059752), and like C-75, the siRNA-targeting FASN downregulated expression of FASN and c-Met proteins as well as inhibited phosphorylation of AKT (Fig. 3B). These data were further confirmed using another FASN-specific siRNA (catalog number SI00059759) targeting a different site of FASN gene to exclude off target effects. Treatment of DLBCL cell lines with cerulenin also downregulated the expression of FASN, c-Met, and p-AKT (data are not shown) as detected by Western blotting, supporting the role of FASN in the regulation of the c-Met and AKT signaling pathway.

Next, we wanted to determine whether FASN is functional upstream of c-Met and AKT pathways. We, therefore, transfected the SUDHL4 cell line with siRNA targeted against c-Met and AKT. As shown in Fig. 3C, neither c-Met or AKT siRNA were able to downregulate

Published OnlineFirst April 27, 2010; DOI: 10.1158/1535-7163.MCT-09-1061

the expression of FASN, however c-Met siRNA transfection caused dephosphorylation of AKT, suggesting that c-Met is upstream of the AKT pathway. As expected, AKT siRNA treatment did not affect the expression of c-Met, confirming that AKT is present downstream of FASN and c-Met. These data confirm that FASN inhibition by C-75 leads to downregulation of c-Met and dephosphorylation of AKT in a sequential manner.

To confirm whether downregulation of FASN leads to induction of apoptosis via the c-Met and AKT pathway, we treated DLBCL cell lines with different concentrations of FASN inhibitor, C-75, c-Met specific inhibitor PHA665752, and PI3-kinase/AKT pathway inhibitor LY294002, either alone or in combination. As shown in Supplementary Fig. S3, C-75 treatment with 10 μM PHA665752 at 500 nM and LY294002 at 5 μM did not induce apoptosis alone; however, when the same doses were used in combination, an appreciable amount of apoptosis was detected after staining the cells with annexin V/PI and analyzed by flow cytometry, suggesting a synergistic effect following combination treatment. These data clearly indicate that FASN inhibition leads to apoptosis via downregulation of the c-Met and PI3-kinase/AKT pathway.

Nuclear translocation of c-Met following FASN inhibition. It has shown that inhibition of FASN leads to nuclear accumulation of RTK p185HER2 in breast cancer (14). To test whether inhibition of FASN mediates the translocation of c-Met into nucleus, SUDHL4 cells were treated with 25 and 50 μM C-75 for 24 hours.

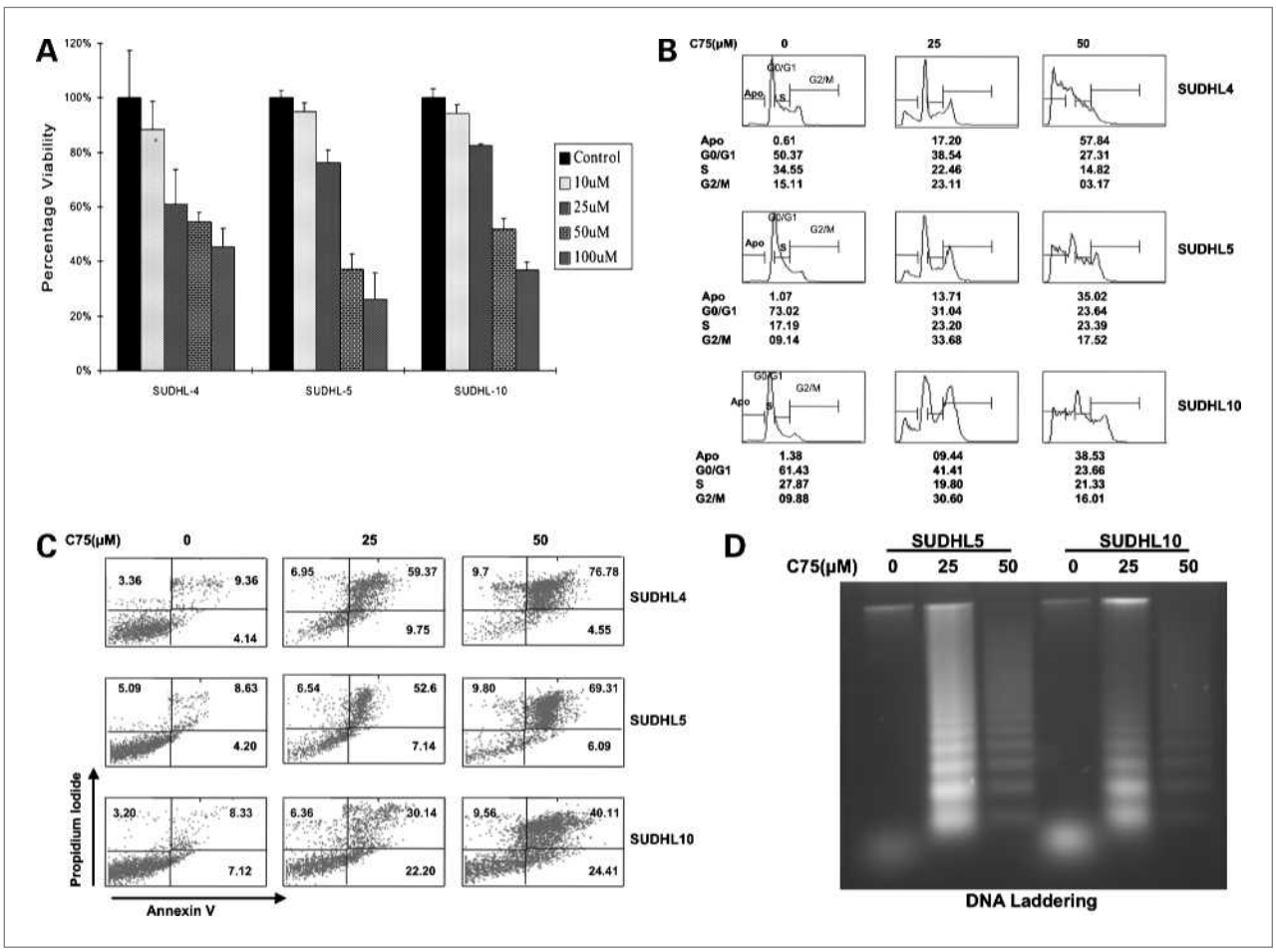

Figure 2. A, C-75 inhibits the proliferation of DLBCL cells. SUDHL4, SUDHL5, and SUDHL10 cells were incubated with DMSO or indicated doses of C-75. Cell proliferation assays were done using MTT as described in Materials and Methods. The graph displays the mean ± standard deviation of three independent experiments with replicates of six wells for all the doses and vehicle control for each experiment; *, $P < 0.01$, statistically significant (Student's *t*-test). B, cell cycle analysis of DLBCL cells following C-75 treatment for 24 hours. SUDHL4, SUDHL5, and SUDHL10 cells were treated with 25 and 50 μM C-75 for 24 hours. Thereafter, the cells were washed, fixed, and stained with propidium iodide, and analyzed for DNA content by flow cytometry as described in Materials and Methods. A representative of four independent experiments is depicted. C, C-75–induced apoptosis detected by annexin V/PI dual staining. SUDHL4, SUDHL5, and SUDHL10 cells were treated with 25 and 50 μM C-75 for 24 hours, and cells were subsequently stained with flourescein-conjugated annexin V and propidium iodide, and apoptotic cells were analyzed by flow cytometry. A representative of four independent experiments is depicted. D, SUDHL5 and SUDHL10 cells were treated with indicated doses of C-75 for 24 hours, cells and DNA were extracted and separated by electrophoresis on 1.5% agarose gel.

Published OnlineFirst April 27, 2010; DOI: 10.1158/1535-7163.MCT-09-1061

Cytoplasmic and nuclear fraction was prepared, and equal amounts of proteins were separated on SDS-PAGE and immunoblotted with antibodies against c-Met. As shown in Fig. 3D, treatment of SUDHL4 cells with C-75 resulted in the accumulation of c-Met into the nucleus.

Inhibition of FASN in DLBCL cells induced apoptosis via the mitochondrial and caspase-mediated pathway. Activated Akt can phosphorylate several apoptosis-regulating proteins including pro-apoptotic Bcl-2 family member BAD (34, 35). BAD promotes cell death by interacting with anti-apoptotic Bcl-2 members such as Bcl-xL, which allows the multidomain pro-apoptotic Bcl-2 family members Bax and Bak to aggregate and cause release of apoptogenic molecules (e.g., cytochrome c) from mitochondria to the cytosol culminating into caspase activation and cell death (36, 37). It has also been shown that

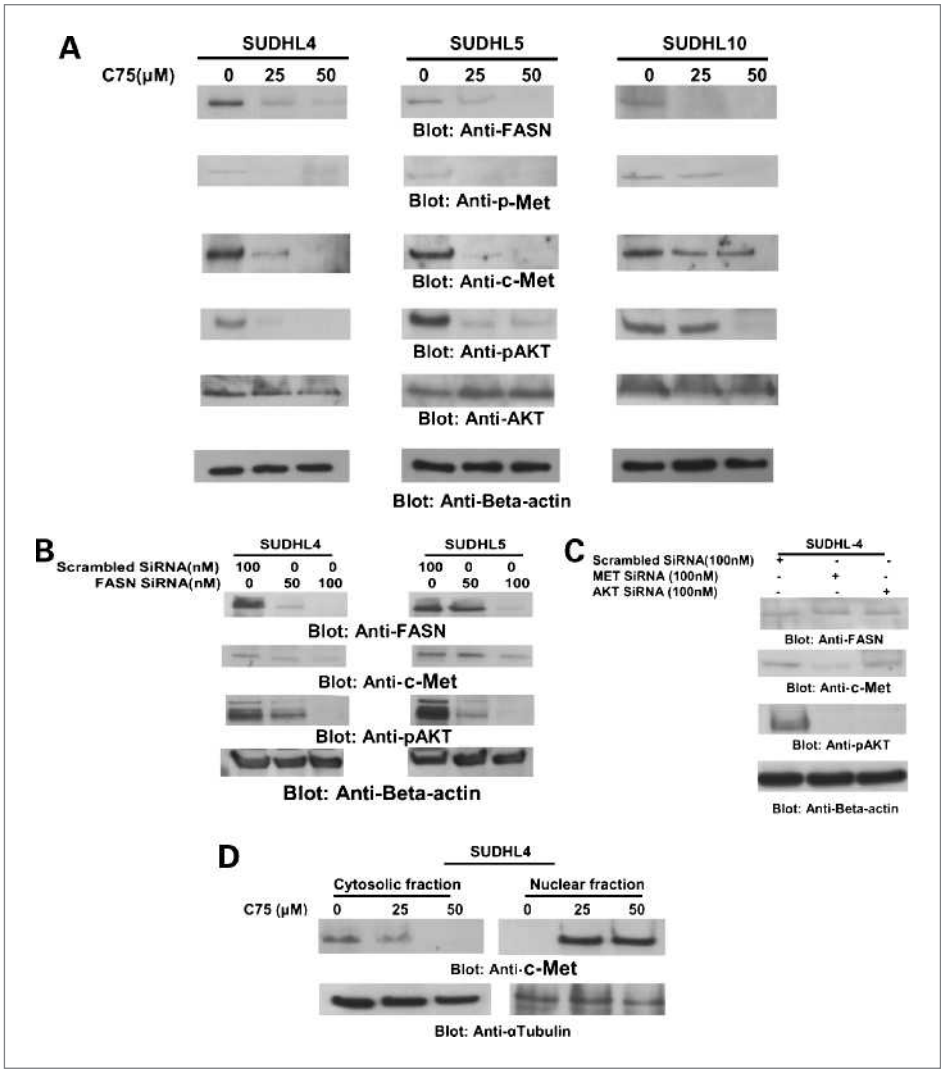

Figure 3. C-75 treatment causes downregulation of FASN, c-Met, and dephosphorylation of constitutive *p*-Met and AKT in DLBCL cell lines. A, C-75 treatment downregulates expression of FASN and c-Met and dephosphorylates c-Met and AKT. SUDHL4, SUDHL5, and SUDHL10 cells were treated with 25 and 50 μM C-75 for 24 hours. After cell lysis, equal amounts of proteins were separated by SDS-PAGE, transferred to immobilon membrane, and immunoblotted with antibodies against FASN, *p*-Met, c-Met, *p*-AKT, AKT, and beta actin as indicated. B, FASN siRNA expression downregulated c-Met and dephosphorylates AKT in DLBCL cell lines. SUDHL4 and SUDHL5 cells were transfected with scrambled siRNA (100 nM) and FASN siRNA (50 and 100 nM) with lipofectamine as described in Materials and Methods. After 48 hours of transfection, cells were lysed and equal amounts of proteins were separated by SDS-PAGE, transferred to immobilon membrane, and immunoblotted with antibodies against FASN, c-Met, *p*-AKT, and beta actin as indicated. C, effect of c-Met and AKT siRNA expression on FASN expression in DLBCL cell lines. SUDHL4 cells were transfected with scrambled siRNA (100 nM), c-Met and AKT siRNA (100 nM) with lipofectamine. After transfection, cells were lysed and equal amounts of proteins were separated by SDS-PAGE, transferred to immobilon membrane, and immunoblotted with antibodies against FASN, c-Met, *p*-AKT, and beta actin as indicated. D, inhibition of FASN expression by C-75 treatment of DLBCL cells translocates c-Met to the nucleus. SUDHL4 cells were treated with 25 and 50 μM C-75 for 24 hours. Cytosolic and nuclear proteins were isolated and proteins were separated by SDS-PAGE, transferred to immobilon membrane, and immunoblotted with antibodies against c-Met and α-tubulin as indicated.

Published OnlineFirst April 27, 2010; DOI: 10.1158/1535-7163.MCT-09-1061

FASN exerts its oncogenic effect by inhibiting the intrinsic pathway of apoptosis (38).

Therefore, in the next series of experiments we sought to determine whether induction of apoptosis via downregulation of FASN and *p*-AKT signaling involves the mitochondrial pathway in DLBCL. We first determined whether inhibition of FASN activate Bax via dephosphorylation of Bad in DLBCL cell lines. As shown in Fig. 4A, treatment of SUDHL5 and SUDHL10 cells with 25 and 50 μM C-75 dephosphorylated Bad in a dose-dependent manner. Inhibition of FASN also led to conformational changes and activation of Bax protein in the SUDHL5 cell line starting at 2 hours after C-75 treatment and peaking at 8 hours (Fig. 4B). We then tested the effect of C-75 on the mitochondrial membrane potential and release of cytochrome c in these cells. Cells were treated with C-75 for 24 hours and labeled with JC1 dye, and mitochondrial membrane potential was measured by flow cytometry. As shown in Fig. 4C, treatment of cells with C-75 resulted in loss of mitochondrial membrane potential in DLBCL cells as measured by JC1-stained green fluorescence depicting apoptotic cells. We then studied the release of cytochrome c from mitochondria into cytosole. As shown in Fig. 4D, a higher level of cytochrome c was measured in cytosolic and lower levels in the mitochondrial fraction in both cell lines after C-75 treatment. These data suggest that C-75 treatment of DLBCL cell lines causes dephosphorylation of Bad leading to activation of the mitochondrial apoptotic pathway.

Release of cytochrome c has been shown to activate the downstream caspases that are ultimately required to induce apoptosis (29–31), we therefore sought to determine whether C-75–induced release of cytochrome c is capable of activation of caspase 9, caspase-3, and PARP. Figure 5A shows that C-75 treatment resulted in the activation of caspase-9, caspase-3, and cleavage of PARP in DLBCL cells after treatment with 25 and 50 μM C-75 for 24 hours. It has been shown that caspase-3 is able to activate caspase-8 and cause Bid cleavage downstream of the mitochondria to achieve the potential the apoptotic stimuli. Our data showed that there was activation of caspase-8 and BID after C-75 treatment (Fig. 5B). In addition, pretreatment of DLBCL cells with 80 μM z-VAD-fmk, a universal inhibitor of caspases, followed by C-75 treatment, abrogated apoptosis and prevented caspase-3 activation induced by C-75 (Supplementary Fig. S4A and B), clearly indicating that caspases play a critical role in C-75–induced apoptosis in DLBCL cells.

Finally, to confirm whether C-75 treatment was specifically targeting caspases-9 and -3 via downregulation of FASN, we did transfection studies with siRNA, specifically targeted against FASN, to determine the status of these proteins in DLBCL cell lines. SUDHL4 and SUDHL5 cells were transfected with FASN-specific siRNA (catalog number SI00059752), and like C-75, the siRNA-targeting FASN downregulated expression of caspases-9 and 3 (Fig. 5C).

Modulation of IAP protein family in C-75–induced apoptosis in DLBCL cells. We also examined whether C-75 induces apoptosis by modulating the expression of inhibitors of apoptosis protein (IAP) family members, which ultimately determine the cell's response to apoptotic stimuli. SUDHL4, SUDHL5, and SUDHL10 cells were treated with 25 and 50 μM C-75 for 24 hours, and expression of cIAP1, XIAP, and survivin were determined using Western blotting. As shown Fig. 5D, C-75 treatment caused a dose-dependent downregulation of cIAP1, survivin, and XIAP. These results indicate that IAP proteins may also be involved in C-75–induced apoptosis.

Discussion

In the light of recent evidence that links FASN activity to RTK activation, including c-Met for the promotion of tumorigenesis in various tumors (39, 40), we sought to explore the relationship between FASN and c-Met expression in a cohort of Saudi DLBCL samples in a TMA format. Our data suggest that there is a significant association between expressions of FASN and c-Met. We further investigated the effect of FASN inhibition on c-Met signaling and found that pharmacological inhibitors of FASN target c-Met phosphorylation and expression, resulting in impaired downstream activity of the PI3-kinase/AKT pathway, leading to inhibition of cell proliferation and induction of apoptosis in DLBCL.

The mechanism by which FASN inhibition decreases c-Met expression is not clear. One possible explanation is that FASN inhibition may cause an imbalance in the membrane phospholipids levels, which may result in decreased c-Met membrane localization and activation (14). This explanation is supported by several lines of evidence. Lipid rafts are membrane microdomains that serve as platforms for cell signaling, and recent studies have revealed a connection between lipid rafts and activity of c-Met (41, 42). Because FASN is the sole enzyme for synthesis of long chain saturated fatty acid and has been shown to maintain membrane microdomain activity, as well as regulate the activity of lipid rafts (8, 43), pharmacological inhibition of FASN might inhibit c-Met expression via disruption of the lipid raft.

Previously, it has been shown that inhibition of FASN leads to the accumulation of Her2 RTK in the nucleus of cancer cells (14). Our results also suggest that inhibition of FASN leads to translocation of c-Met RTK in the nucleus of DLBCL cells, indicating that FASN signaling modulates not only the expression of c-Met but also its nuclear localization.

Because the bulk of endogenously synthesized fatty acids are incorporated into membrane lipids by proliferating tumor cells (44), pharmacological FASN blockade might result in rapid changes in the lipid composition of the tumor cell membrane, which could impair a correct cellular localization of c-Met. Cerulenin and C-75 may promote c-Met to enter the nucleus and to induce transcriptional activation of c-Met genes.

Published OnlineFirst April 27, 2010; DOI: 10.1158/1535-7163.MCT-09-1061

In our large cohort of DLBCL samples, the overexpression of FASN in 62.6% and c-Met in 73.2%, and the highly significant association between FASN and c-Met, are additional confirmation of the pathogenic role of both of these markers in the tumorigenesis of Middle Eastern DLBCL and their potential biological link. Furthermore, previous studies have shown that overexpression of either HGF or c-Met in DLBCL tumor sections, as well as high levels of HGF in the serum of DLBCL patients, has been associated with poor prognosis (17, 18). More recently, a gene profiling study showed significantly enhanced expression of c-Met upon transformation of low follicular grade into DLBCL within the same patients, which suggests a pathogenic role of c-Met RTK in DLBCL. However, surprisingly in our study of DLBCL, c-Met overexpression is found to have good prognostic significance (P = 0.0028). This association with better survival remains significant even in a multivariant analysis, thereby confirming c-Met as an independent prognostic marker for better outcome in DLBCL. It might be paradoxical that DLBCL-containing receptors for tyrosine kinase such as c-Met had a better prognosis as compared with tumors without c-Met expression. One speculation could be that lymphoma cells with c-Met have retained the physiological growth control by c-Met, which is supported by the strong link between c-Met and the DLBCL GC subtype. Another factor that can attribute the favorable outcome in DLBCL expressing c-Met is the significant association with high proliferative index Ki67 (P = 0.0012), which might result in cell cycle progression and possibly chemotherapy sensitivity. Interestingly, previous studies in other Non-Hodgkin's lymphomas, like follicular lymphoma, have shown that tumors with more proliferating cells respond better to chemotherapy and have better

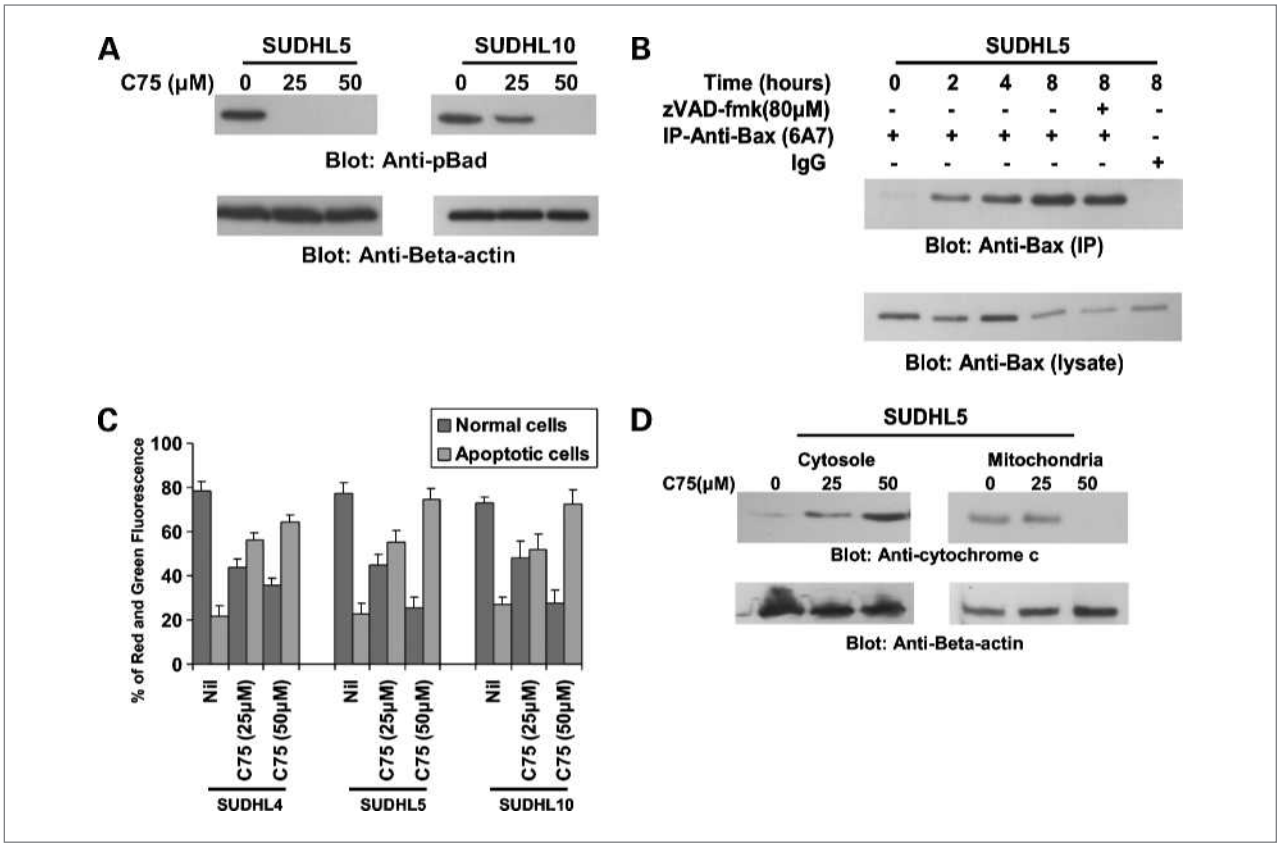

Figure 4. C-75–induced mitochondrial apoptotic pathway in DLBCL cells. A, C-75 treatment causes dephosphorylation of Bad pro-apoptotic protein. SUDHL5 and SUDHL10 cells were treated with 25 and 50 μM C-75 for 24 hours. Cells were lysed and proteins were immunoblotted with antibodies against anti-*p*Bad and beta-actin. B, C-75–induced Bax activation in DLBCL cells. After treating with 50 μM C-75 for 2, 4, and 8 hours as indicated, SUDHL4 cells were lysed in 1% chaps lysis buffer and subjected to immunoprecipitation with either anti-Bax 6A7 antibody or nonspecific immunoglobulin G for detection of conformationally changed Bax protein. In addition, the total cell lysates were applied directly to SDS-PAGE, transferred to immobilon membrane, and immunoblotted with specific anti-Bax polyclonal antibody. C, loss of mitochondrial potential by C-75 treatment of DLBCL cells. SUDHL4, SUDHL5, and SUDHL10 cells were treated with and without 25 and 50 μM C-75 for 24 hours. Live cells with intact mitochondrial membrane potential (dark gray bars) and dead cells with lost mitochondrial membrane potential (light gray bars) were measured by JC-1 staining and analyzed by flow cytometry as described in Materials and Methods. An average of three independent experiments is depicted. D, C-75–induced release of cytochrome c. SUDHL5 cells were treated with and without 25 and 50 μM C-75 for 24 hours. Mitochondrial-free cytosolic fractions as well as mitochondrial extracts were isolated as described in Materials and Methods. Cell extracts were separated on SDS-PAGE, transferred to PVDF membrane, and immunoblotted with an antibody against cytochrome c. Beta-actin was used for equal loading.

Published OnlineFirst April 27, 2010; DOI: 10.1158/1535-7163.MCT-09-1061

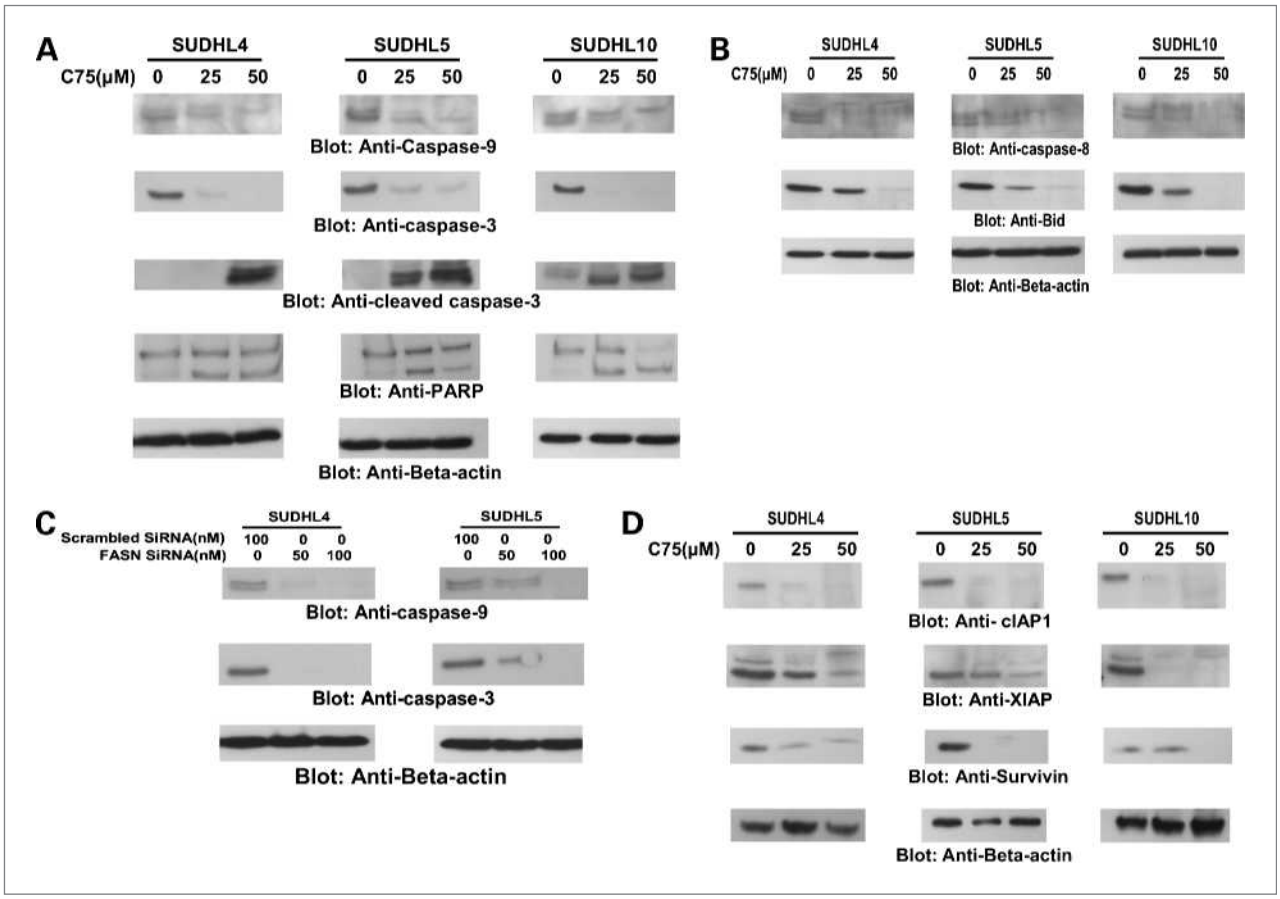

Figure 5. Activation of caspases induced by C-75 treatment in DLBCL cells. SUDHL4, SUDHL5, and SUDHL10 cells were treated with and without 25 and 50 μM C-75 for 24 hours. Cells were lysed and proteins were immunoblotted with antibodies against caspase-9, pro-caspase-3, cleaved caspase-3, PARP, and beta-actin. Each experiment was repeated three times to confirm reproducibility. B, activation of caspase-8 and truncation of Bid induced by C-75 treatment in DLBCL cells. SUDHL4, SUDHL5, and SUDHL10 cells were treated with and without 25 and 50 μM C-75 for 24 hours. Cells were lysed and proteins were immunoblotted with antibodies against caspase-8, Bid, and beta-actin. Each experiment was repeated three times to confirm reproducibility. C, FASN siRNA expression downregulated caspases-9 and -3 in DLBCL cell lines. SUDHL4 and SUDHL5 cells were transfected with scrambled siRNA (100 nM) and FASN siRNA (50 and 100 nM) with lipofectamine as described in Materials and Methods. After 48 hours of transfection, cells were lysed and equal amounts of proteins were separated by SDS-PAGE, transferred to immobilon membrane, and immunoblotted with antibodies against caspase-9, caspase-3, and beta actin as indicated. D, C-75–induced downregulation of cIAP1, XIAP, and survivin expression. SUDHL4, SUDHL5, and SUDHL10 cells were treated with and without 25 and 50 μM C-75 for 24 hours. Cells were lysed and equal amounts of proteins were separated on SDS-PAGE, transferred to PVDF membrane, and immunoblotted with antibodies against cIAP1, XIAP, survivin, and beta-actin as indicated.

survival (45, 46). This hypothesis is supported by our data, which show that FASN inhibition prevents cell proliferation and induces mitochondrial and caspase-dependent apoptosis in DLBCL cell lines. On the other hand, C-75 treatment of normal peripheral blood mononuclear cells failed to induce apoptosis because of a lack of FASN expression (12). The predictive value of c-Met in our study is conflicting with results of Kawana (20) in which they found DLBCL expressing c-Met had a worse outcome. The reason behind this discrepancy is not clear. However, the difference in the sample size, ethnic origin, the use of a different methodology of IHC analysis (TMA versus large sections), and different scoring system might be contributing factors.

The identification of c-Met autophosphorylation and subsequent signaling through the PI3K pathway as a target for FASN inhibitors in DLBCL was unexpected but makes sense, as the results presented in the current study suggest that the activity of the PI3K pathway was partly driven by the basal c-Met activity. In addition, expression of c-Met was not regulated by the PI3K/AKT pathway because inhibition of PI3K/AKT did not induce any c-Met loss.

Our study shows that tumor cells in DLBCL respond to FASN inhibition by the specific suppression of the c-Met oncogene, which might provide a molecular rationale to the design of novel therapies directed against FASN in c-Met overexpressing DLBCL.

Disclosure of Potential Conflicts of Interest

No potential conflicts of interest were disclosed.

Published OnlineFirst April 27, 2010; DOI: 10.1158/1535-7163.MCT-09-1061

Acknowledgments

The costs of publication of this article were defrayed in part by the payment of page charges. This article must therefore be hereby marked *advertisement* in accordance with 18 U.S.C. Section 1734 solely to indicate this fact.

Received 11/18/2009; revised 03/03/2010; accepted 03/05/2010; published OnlineFirst 04/27/2010.

References

1. Savage KJ, Shipp MA. Initial evaluation: staging and prognostic factors. In: Mauch LP, Armitage J, Harris N, Dalla-Favera R, Coiffer B, editors. Non-Hodgkin's lymphomas. Philadelphia (PA): Lippincott Williams and Wilkins; 2004, p. 97–125.
2. Asturias FJ, Chadick JZ, Cheung IK, et al. Structure and molecular organization of mammalian fatty acid synthase. Nat Struct Mol Biol 2005;12:225–32.
3. Wakil SJ. Fatty acid synthase, a proficient multifunctional enzyme. Biochemistry 1989;28:4523–30.
4. Milgraum LZ, Witters LA, Pasternack GR, Kuhajda FP. Enzymes of the fatty acid synthesis pathway are highly expressed in *in-situ* breast carcinoma. Clin Cancer Res 1997;3:2115–20.
5. Uddin S, Siraj AK, Al-Rasheed M, et al. Fatty acid synthase and AKT pathway signaling in a subset of papillary thyroid cancers. J Clin Endocrinol Metab 2008;93:4088–97.
6. Kuhajda FP. Fatty-acid synthase and human cancer: new perspectives on its role in tumor biology. Nutrition 2000;16:202–8.
7. Kuhajda FP. Fatty acid synthase and cancer: new application of an old pathway. Cancer Res 2006;66:5977–80.
8. Wang HQ, Altomare DA, Skele KL, et al. Positive feedback regulation between AKT activation and fatty acid synthase expression in ovarian carcinoma cells. Oncogene 2005;24:3574–82.
9. Pizer ES, Pflug BR, Bova GS, Han WF, Udan MS, Nelson JB. Increased fatty acid synthase as a therapeutic target in androgen-independent prostate cancer progression. Prostate 2001;47:102–10.
10. Baron A, Migita T, Tang D, Loda M. Fatty acid synthase: a metabolic oncogene in prostate cancer? J Cell Biochem 2004;91:47–53.
11. Menendez JA, Lupu R. Fatty acid synthase and the lipogenic phenotype in cancer pathogenesis. Nat Rev Cancer 2007;7:763–77.
12. Pizer ES, Wood FD, Pasternack GR, Kuhajda FP. Fatty acid synthase (FAS): a target for cytotoxic antimetabolites in HL60 promyelocytic leukemia cells. Cancer Res 1996;56:745–51.
13. Wang WQ, Zhao XY, Wang HY, Liang Y. Increased fatty acid synthase as a potential therapeutic target in multiple myeloma. J Zhejiang Univ Sci B 2008;9:441–7.
14. Menendez JA, Vellon L, Mehmi I, et al. Inhibition of fatty acid synthase (FAS) suppresses HER2/neu (erbB-2) oncogene overexpression in cancer cells. Proc Natl Acad Sci U S A 2004;101:10715–20.
15. Coleman DT, Bigelow R, Cardelli JA. Inhibition of fatty acid synthase by luteolin post-transcriptionally down-regulates c-Met expression independent of proteosomal/lysosomal degradation. Mol Cancer Ther 2009;8:214–24.
16. van der Voort R, Taher TE, Derksen PW, et al. The hepatocyte growth factor/Met pathway in development, tumorigenesis, and B-cell differentiation. Adv Cancer Res 2000;79:39–90.
17. Hsiao LT, Lin JT, Yu IT, et al. High serum hepatocyte growth factor level in patients with non-Hodgkin's lymphoma. Eur J Haematol 2003;70:282–9.
18. Kawano R, Ohshima K, Karube K, et al. Prognostic significance of hepatocyte growth factor and c-Met expression in patients with diffuse large B-cell lymphoma. Br J Haematol 2004;127:305–7.
19. Abubaker J, Jehan Z, Bavi P, et al. Clinicopathological analysis of papillary thyroid cancer with PIK3CA alterations in a Middle Eastern population. J Clin Endocrinol Metab 2008;93:611–8.
20. Jaffe ES, Harris NL, Stein H, Vardiman JW. World Health Organization Classification of Tumors: Pathology and Genetics of Tumors of Hematopoietic and Lymphoid Tissues. Lyon: IARC; 2001.
21. Bavi P, Jehan Z, Atizado V, et al. Prevalence of fragile histidine triad expression in tumors from Saudi Arabia: a tissue microarray analysis. Cancer Epidemiol Biomarkers Prev 2006;15:1708–18.
22. McCarty KS, Jr., Miller LS, Cox EB, et al. Estrogen receptor analyses. Correlation of biochemical and immunohistochemical methods using monoclonal antireceptor antibodies. Arch Pathol Lab Med 1985;109:716–21.
23. Uddin S, Hussain AR, Siraj AK, et al. Role of phosphatidylinositol 3'-kinase/AKT pathway in diffuse large B-cell lymphoma survival. Blood 2006;108:4178–86.
24. Abubaker J, Bavi P, Al-Harbi S, et al. Clinicopathological analysis of colorectal cancers with PIK3CA mutations in Middle Eastern population. Oncogene 2008;27:3539–45.
25. Uddin S, Hussain AR, Ahmed M, et al. S-phase kinase protein 2 is an attractive therapeutic target in a subset of diffuse large B cell lymphoma. J Pathol 2008;216:483–94.
26. Hans CP, Weisenburger DD, Greiner TC, et al. Confirmation of the molecular classification of diffuse large B-cell lymphoma by immunohistochemistry using a tissue microarray. Blood 2004;103:275–82.
27. Bavi P, Abubaker J, Hussain A, et al. Reduced or absent cyclin H expression is an independent prognostic marker for poor outcome in diffuse large B-cell lymphoma. Hum Pathol 2008;39:885–94.
28. Hussain AR, Al-Rasheed M, Manogaran PS, et al. Curcumin induced apoptosis in Acute T cell Leukemia. Apoptosis 2006;11:245–54.
29. Hussain AR, Al-Jomah NA, Siraj AK, et al. Sanguinarine-dependent induction of apoptosis in primary effusion lymphoma cells. Cancer Res 2007;67:3888–97.
30. Uddin S, Hussain AR, Manogaran PS, et al. Curcumin suppresses growth and induces apoptosis in primary effusion lymphoma. Oncogene 2005;24:7022–30.
31. Hussain AR, Ahmed M, Al-Jomah NA, et al. Curcumin suppresses constitutive activation of nuclear factor-kappa B and requires functional Bax to induce apoptosis in Burkitt's lymphoma cell lines. Mol Cancer Ther 2008;7:3318–29.
32. Uddin S, Ah-Kang J, Ulaszek J, et al. Differentiation stage-specific activation of p38 mitogen-activated protein kinase isoforms in primary human erythroid cells. Proc Natl Acad Sci U S A 2004;101:147–52.
33. Uddin S, Hussain AR, Al-Hussein KA, et al. Inhibition of phosphatidylinositol 3'-kinase/AKT signaling promotes apoptosis of primary effusion lymphoma cells. Clin Cancer Res 2005;11:3102–8.
34. del Peso L, González-García M, Page C, Herrera R, Nuñez G. Interleukin-3-induced phosphorylation of BAD through the protein kinase Akt. Science 1997;278:687–9.
35. Shin I, Bakin AV, Rodeck U, Brunet A, Arteaga CL. Transforming growth factor beta enhances epithelial cell survival via Akt-dependent regulation of FKHRL1. Mol Biol Cell 2001;12:3328–39.
36. Wei MC, Zong WX, Cheng EH, et al. Proapoptotic BAX and BAK: a requisite gateway to mitochondrial dysfunction and death. Science 2001;292:727–30.
37. Ho TS, Ho YP, Wong WY, et al. Fatty acid synthase inhibitors Cerulenin and C75 retard growth and induce caspase-dependent apoptosis in human melanoma A-375 cells. Biomed Pharmacother 2007;61:578–87.
38. Migita T, Ruiz S, Fornari A, et al. Fatty acid synthase: a metabolic enzyme and candidate oncogene in prostate cancer. J Natl Cancer Inst 2009;101:519–32.
39. Tjin EP, Groen RW, Vogelzang I, et al. Functional analysis of HGF/c-Met signaling and aberrant HGF-activator expression in diffuse large B-cell lymphoma. Blood 2006;107:760–8.
40. Brusselmans K, Vrolix R, Verhoeven G, Swinnen JV. Induction of cancer cell apoptosis by flavonoids is associated with their ability

Published OnlineFirst April 27, 2010; DOI: 10.1158/1535-7163.MCT-09-1061

to inhibit fatty acid synthase activity. J Biol Chem 2005;280:5636–45.
41. Huo H, Guo X, Hong S, Jiang M, Liu X, Liao K. Lipid rafts/caveolae are essential for insulin-like growth factor-1 receptor signaling during 3T3–1 preadipocyte differentiation induction. J Biol Chem 2003;278:11561–9.
42. Wang L, Zhao YF, Li YL, Xu YF, Xia Q, Ma KL. Effects of lipid rafts on signal transmembrane transduction mediated by c-Met. Zhonghua Gan Zang Bing Za Zhi 2008;16:449–52.
43. Swinnen JV, Van Veldhoven PP, Timmermans L, et al. Fatty acid synthase drives the synthesis of phospholipids partitioning into detergent-resistant membrane microdomains. Biochem Biophys Res Commun 2003;302:898–903.
44. Pizer ES, Jackisch C, Wood FD, et al. Inhibition of fatty acid synthesis induces programmed cell death in human breast cancer cells. Cancer Res 1996;56:2745–7.
45. Björck E, Ek S, Landgren O, et al. High expression of cyclin B1 predicts a favorable outcome in patients with follicular lymphoma. Blood 2005;105:2908–15.
46. Wilson WH, Teruya-Feldstein J, Fest T, et al. Relationship of p53, bcl-2, and tumor proliferation to clinical drug resistance in non-Hodgkin's lymphomas. Blood 1997;89:601–9.

Published OnlineFirst April 27, 2010; DOI: 10.1158/1535-7163.MCT-09-1061

Molecular Cancer Therapeutics

Inhibition of Fatty Acid Synthase Suppresses c-Met Receptor Kinase and Induces Apoptosis in Diffuse Large B-Cell Lymphoma

Shahab Uddin, Azhar R. Hussain, Maqbool Ahmed, et al.

Mol Cancer Ther 2010;9:1244-1255. Published OnlineFirst April 27, 2010.